JACS Au
AN OPEN ACCESS JOURNAL OF THE AMERICAN CHEMICAL SOCIETY

pubs.acs.org/jacsau
Article

Opposed Aromatic Surfaces Behave as Independent Binding Sites for Carbohydrate Stacking: Analysis of Sandwich-like CH/π/CH Complexes

Laura Díaz-Casado, Enrique Mann, Ester Jiménez-Moreno, Alejandro Villacampa, Laura Montalvillo-Jiménez, Claudia Sánchez-García, Francisco Corzana, Jesús Jiménez-Barbero, Ana María Gómez, Andrés G. Santana, and Juan Luis Asensio*

Cite This: JACS Au 2024, 4, 4466−4473
Read Online

ACCESS | Metrics & More | Article Recommendations | Supporting Information

ABSTRACT: CH/π bonds are versatile elements for the construction of complex molecular architectures, thus playing key roles in many biomolecular recognition processes. Although seldom acknowledged, aromatic units are inherently bivalent and can participate in CH/π bonds through either face simultaneously, leading to the formation of *ternary* stacking complexes. This sandwich-like arrangement is by far the most common in natural complexes and could potentially lead to negative cooperativity due to unfavorable polarization or electrostatic effects, especially when polarized CH fragments are involved. To evaluate the energetics of such interaction modes, we selected a biologically relevant model, *carbohydrate/aromatic stacking*, and conducted an experimental analysis comparing *binary* CH/π interactions to *ternary* CH/π/CH stacking. Our approach utilized a dynamic combinatorial strategy, which is well-suited to reveal minor stability differences among aromatic complexes. Our results showed that carbohydrate/aromatic stacking is relatively insensitive to molecular recognition events occurring on the opposite side of the aromatic platform, whether exposed to water or involved in additional CH/π contacts, with free energy fluctuations lower than 10%. Based on these data, for all practical purposes, the two opposing aromatic surfaces can be considered independent, noninteracting binding sites, making aromatic platforms optimal connecting elements for supramolecular cross-linking.

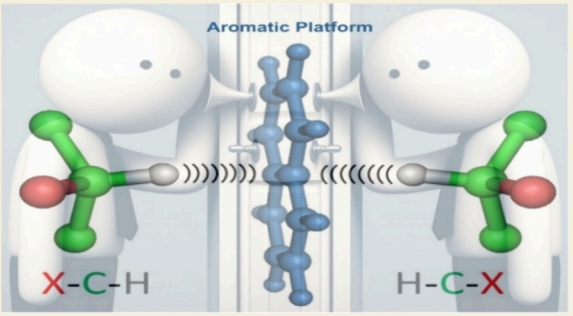

KEYWORDS: *molecular recognition, dynamic covalent chemistry, reductive amination, equilibrium, sandwich-type, CH/π ternary complexes, cooperativity, NMR*

INTRODUCTION

Aromatic units are versatile molecular recognition elements, capable of participating in a wide variety of noncovalent interactions with both neutral and charged partners.[1,2] Among these, CH/π interactions are ubiquitous in biomolecular complexes[3−7] and play crucial roles in supramolecular,[8,9] medicinal,[10,11] and polymer chemistry,[12,13] as well as in catalysis.[14,15] These interactions are considered a type of nonconventional hydrogen bond, involving a polarized CH fragment (soft acid) and a π-cloud (soft base). Traditionally, CH/π interactions have been analyzed in the context of binary CH-donor/aromatic complexes.[3] However, aromatic units are inherently bivalent, capable of interacting with multiple CH/π donors through their two opposing faces simultaneously (Figure 1). Indeed, these ternary arrangements are highly common in proteins and ligand/protein complexes.[4,16] Aromatic units within protein hydrophobic cores are often sandwiched between aliphatic or aromatic CH fragments. Similarly, molecular recognition epitopes formed by tryptophan or tyrosine residues are frequently preorganized by intramolecular CH/π contacts. A prime example of this is seen in carbohydrate/aromatic complexes, where certain aromatic residues establish simultaneous CH/π bonds with both the glycosidic ligand and another protein residue (Figure 1).[17]

Molecular recognition processes typically involve various intermolecular noncovalent interactions, whose influence on complex stability is often not directly additive due to cooperativity effects.[18,19] One well-studied example is the mutual reinforcement of hydrogen bonds within hydrogen bonding networks, which can increase stability by up to 3.3 kcal/mol.[20] More recently, it has been shown that aromatic

Received: August 30, 2024
Revised: October 2, 2024
Accepted: October 4, 2024
Published: October 14, 2024

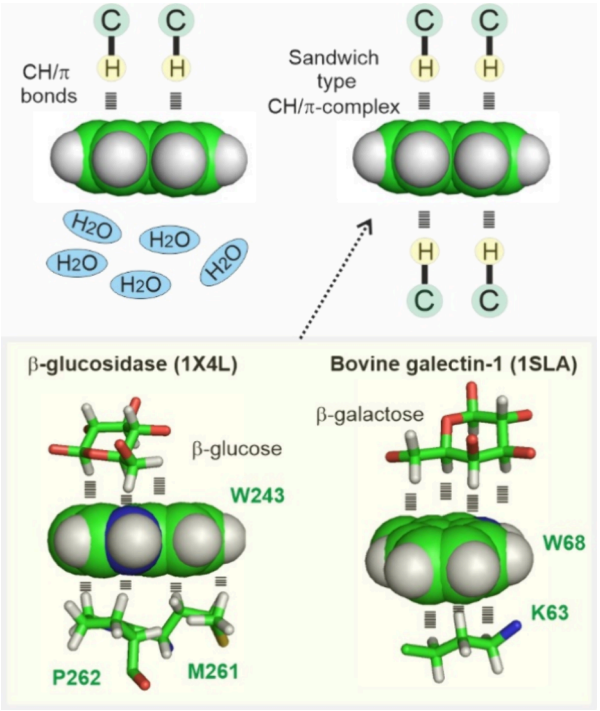

Figure 1. Schematic representation of binary (left) and ternary (right) CH/π complexes (top). These sandwich-like arrangements are common in protein/carbohydrate complexes (bottom).

interactions can also benefit from cooperativity effects, with a notable increase in π/π stacking energy in the presence of ions.[21,22] Cation/π interactions are similarly enhanced by π/π contacts, though to a lesser extent.[21] Still, the question whether this also applies to nonconventional CH/π bonds remains; on the one hand, they are primarily dominated by dispersive forces, and therefore are expected to be relatively insensitive to such influences. However, electrostatic contributions can significantly modulate these interactions too. Thus, depending on the complex geometry, mutual reinforcement or interference between contacts cannot be ruled out. In particular, the formation of sandwich-type ternary complexes with the aromatic platform in the middle may lead to anticooperative effects, potentially due to polarization of the π-cloud or to secondary electrostatic repulsion between interacting CH fragments or heteroatoms on either end. Despite the extensive analysis of cooperativity in classical hydrogen bonds, experimental studies on CH/π interactions remain scarce.[18,19] Reported examples are limited to specific arrangements involving several CH fragments and a single face of the aromatic unit, where positive cooperativity has been observed, as the stability contribution of each contact increases with more interactions.[23] Conversely, sandwich-type complexes mediated by opposite aromatic faces, though common in nature, have been largely overlooked by the chemical community. This is understandable, as experimentally analyzing such systems is challenging and requires not only suitable model systems but also the ability to detect minor stability differences. Herein, we set out to analyze the stability of both *binary* and sandwich-type *ternary* interactions in water (Figure 1, top-left and top-right, respectively).

RESULTS

To tackle the potential stability differences between binary and ternary complexes, we focused our attention on a particular type of CH/π complex of biological relevance, namely carbohydrate/aromatic stacking,[17,24,25] and resorted to an updated version of a strategy previously developed by us.[26−28] Our approach, based on the principles of dynamic combinatorial chemistry,[29,30] is ideally suited to reveal subtle energy differences between interaction modes, and involves the preparation of several 3-amino-sugar derivatives and aromatic-containing aldehydes (Figure 2a). More specifically, we designed and synthesized 1,3-diaxial amino-glycoside models **1**−**4** and aldehydes **a1**−**a3**. Derivatives **1**−**4** comprise a reactive 3-amino-3-deoxy-α-D-altro-pyranose linked to different CH/π donor glycosides (**2**−**4**) or to a reference ethylene glycol fragment (**1**) as aglycon. On the other hand, aldehydes **a1**−**a3** contain a naphthyl unit that has been derivatized with fragments of increasing complexity: while both aromatic faces are solvent-exposed in **a1**−**a2**, in the case of **a3** the naphthyl ring already bears a β-galactopyranose cargo which participates in a stable galactose/aromatic complex through the α face (Figure S1). In order to derive the stability of the *binary* carbohydrate/aromatic complexes (Figure 2b, top), we performed pairwise competition experiments at 25 °C in which buffered aqueous solutions containing equimolecular **1**/**2**, **1**/**3** or **1**/**4** mixtures were treated with a substoichiometric amount of aldehydes **a1** or **a2** to form a dynamic mixture of hemiaminals/imines/enamines in exchange (herein named by combining the parent amino-glycoside and aldehyde notations, i.e., **2-a1**, **3-a2**, etc.).

According to our experience,[26−28] adducts derived from **2**−**4** present an intramolecular stacking involving the napthyl ring and the α or β face of the corresponding CH/π donor pyranoses. Thus, while the β-galactose or β-fluoro-mannose units present in **2** and **3**, respectively, lie on their α-face, the α-glucopyranose in **4** forms a β-type complex. On the contrary, no stacking is feasible in species generated from **1**, which was employed as reference. As a consequence of the newly established contacts, imine pairs exhibit dissimilar stabilities and equilibrium populations, rendering after chemical reduction a nonequimolecular mixture of secondary amines (named as the parent imines but with capital letters, i.e., **2-A1**, **3-A2**, etc.). These relative populations, evaluated by NMR, allowed determining the interaction free energies of the different carbohydrate/aromatic complexes (ΔG_{binary}).

Stability values for the CH/π contacts in the context of a ternary carbohydrate/aromatic/carbohydrate complex ($\Delta G_{ternary}$) were derived employing an identical procedure with aldehyde **a3** (Figure 2b, bottom). As a final step, ΔG_{binary} and $\Delta G_{ternary}$ values were compared to reveal any cooperativity effects between stacked glycosides within the sandwich-like arrangement.

Figure 3a shows final amine populations obtained after pairwise competition experiments performed with mixtures **1**/**2**, **1**/**3** or **1**/**4** (from top to bottom), employing a substoichiometric amount of aldehydes **a1**, **a2** or **a3** (from left to right). Population ratios, together with the inferred ΔG values at 25 °C are also shown (see also Table S1). Thus, it can be observed that reactions performed with pair **1**/**2** and aldehyde **a1** yielded reduced products **1-A1** and **2-A1** in a 4.4 ratio, consistent with a stability of 0.87 kcal/mol for the galactose/naphthyl stacking. Results with aldehyde **a2**

https://doi.org/10.1021/jacsau.4c00795
JACS Au 2024, 4, 4466−4473

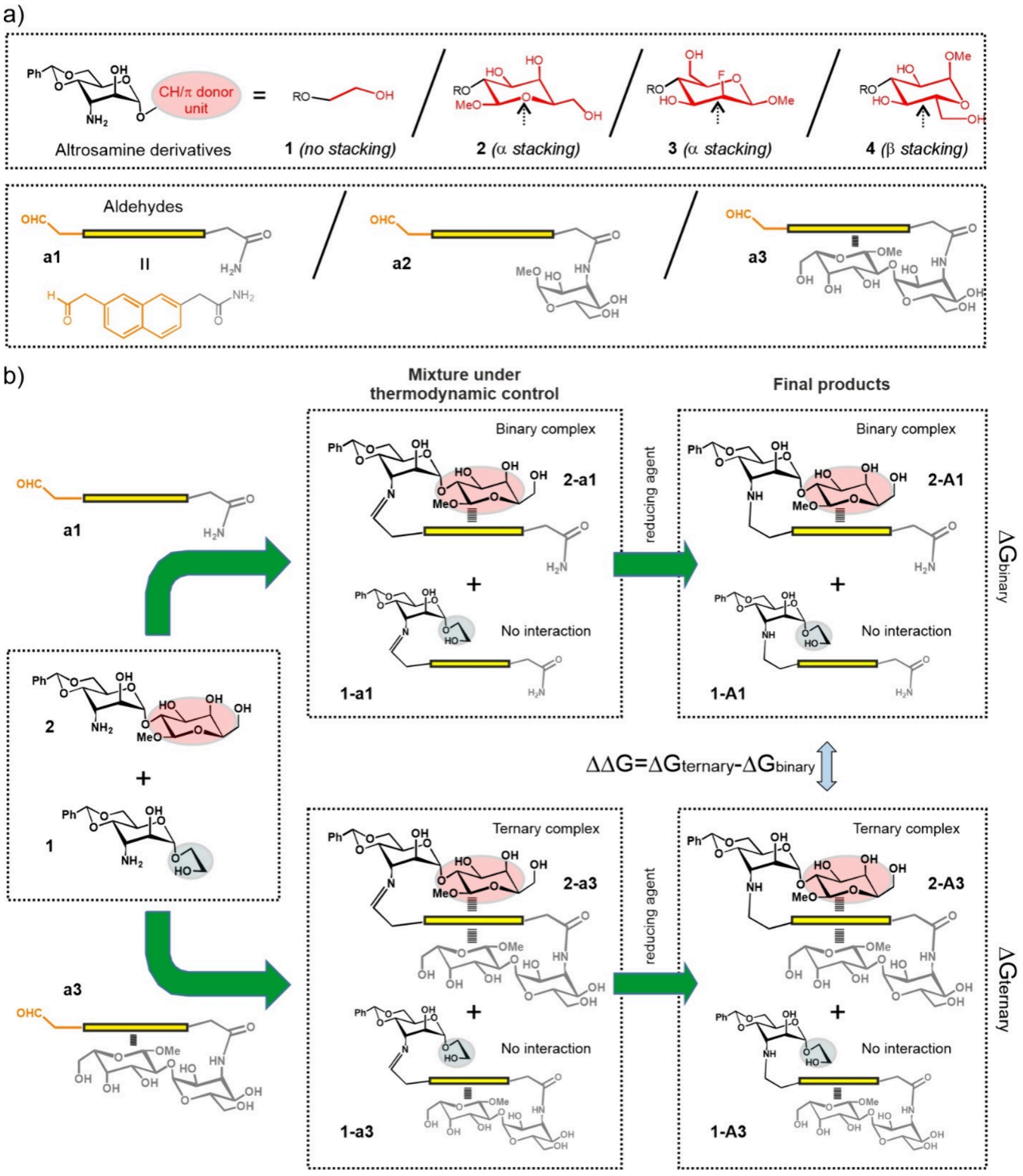

Figure 2. (a) Library of altrosamine models **1**−**4** (top) and aldehydes **a1**−**a3** (bottom) employed for the study of facial cooperativity effects in stacking complexes. (b) Schematic representation of the dynamic combinatorial approach used to this end (see the main text). Adduct populations are too low for NMR detection. Therefore, imine structures were selected for illustrative purposes as the reduction step must inevitably involve these species.

paralleled those previously obtained (product ratio R = 4.8 and ΔG = 0.92 kcal/mol), further supporting the free energy value derived for the binary complex. Interestingly, reactions performed with aldehyde **a3** showed that the stability of the galactose/naphthyl CH/π contacts in a galactose/naphthyl/galactose ternary complex was almost identical to those described for the binary interactions (product ratio R = 4.7, ΔG = 0.91 kcal/mol). Indeed, all the observed free energies fall within the range ΔG = 0.9 ± 0.03 kcal/mol implying a ±3.3% variation with respect to the average and a maximal difference

https://doi.org/10.1021/jacsau.4c00795
JACS Au 2024, 4, 4466−4473

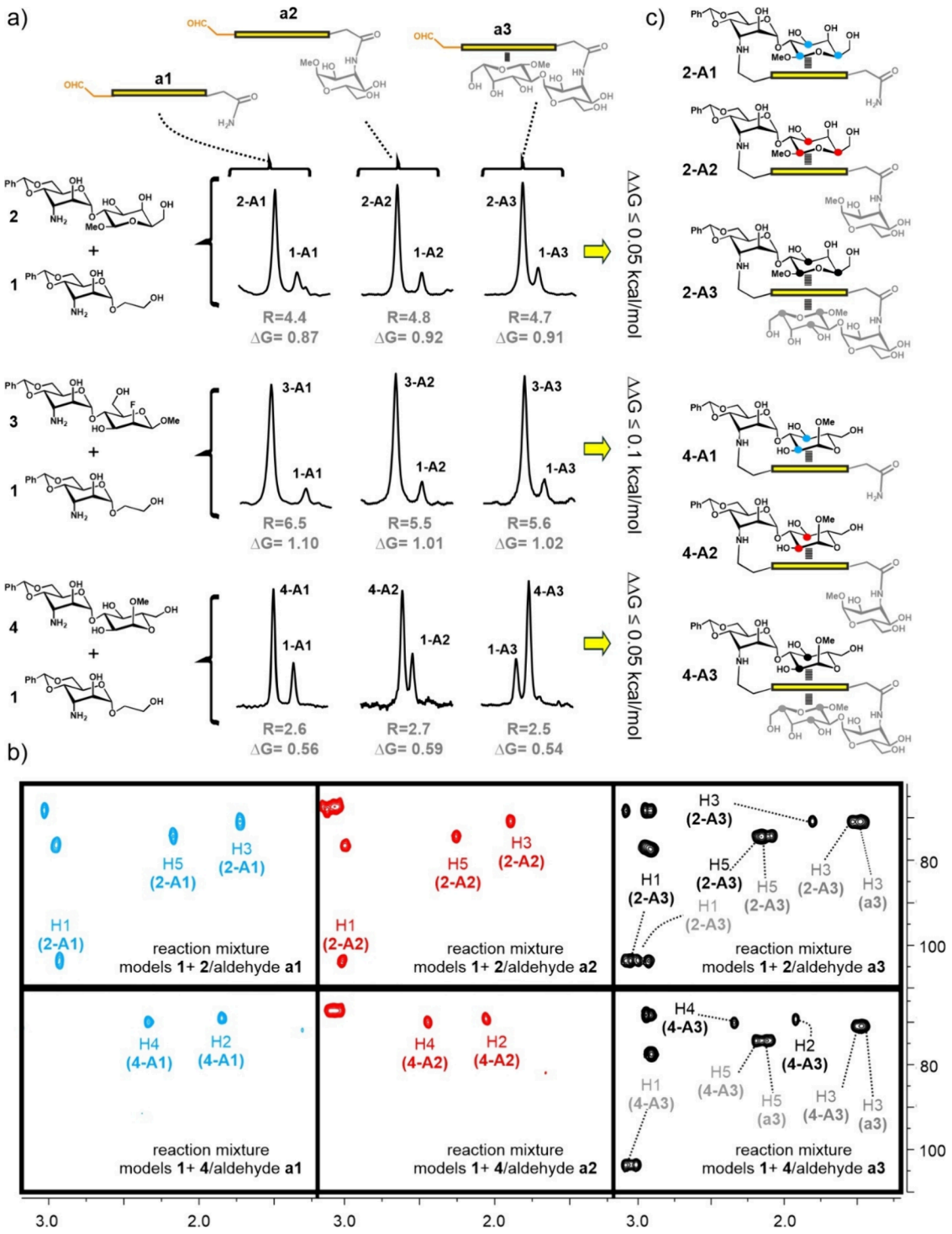

Figure 3. (a) Competition experiments performed in NMR tubes with pairs **1**/**2** (top), **1**/**3** (middle panel) and**1**/**4** (bottom) employing aldehydes **a1**, **a2** and **a3** (from left to right). Key signals of the final adducts (corresponding to the benzylidene CH proton) are represented in every case, together with the estimated product ratios (*R*) and derived free energy values (kcal/mol). (b) HSQC data sets obtained from pairs **2**/**1** (top) and **4**/**1** (bottom) after reaction with aldehydes **a1** (cyan), **a2** (red) and **a3** (black and gray). (c) Stacking interactions in adducts **2-A1**, **2-A2**, **2-A3** (top) and **4-A1**, **4-A2**, **4-A3** (bottom) are shown.

of 0.05 kcal/mol between individual values. Similar results were obtained with **1**/**3** and **1**/**4** pairwise competitions. More specifically, the slightly enhanced strength of the fluoro-mannose/naphthyl interaction established within adducts **3** was in the 1.05 ± 0.05 kcal/mol range, either in the context of the binary or ternary complexes, with max. differences amounting to 0.1 kcal/mol (adducts **3-A1** vs **3-A2**, Figure 3a). Finally, the glucose/naphthyl stacking formed in secondary amines **4** displayed a more reduced stability, the expected behavior for an interaction involving the endocyclic oxygen of the pyranose *β*-face.[27] However, as observed with the previous models, obtained free energies were almost identical in all cases, being all values within the 0.56 ± 0.03 kcal/mol range and a max. difference of 0.05 kcal/mol (**4-A2**

https://doi.org/10.1021/jacsau.4c00795
JACS Au 2024, 4, 4466−4473

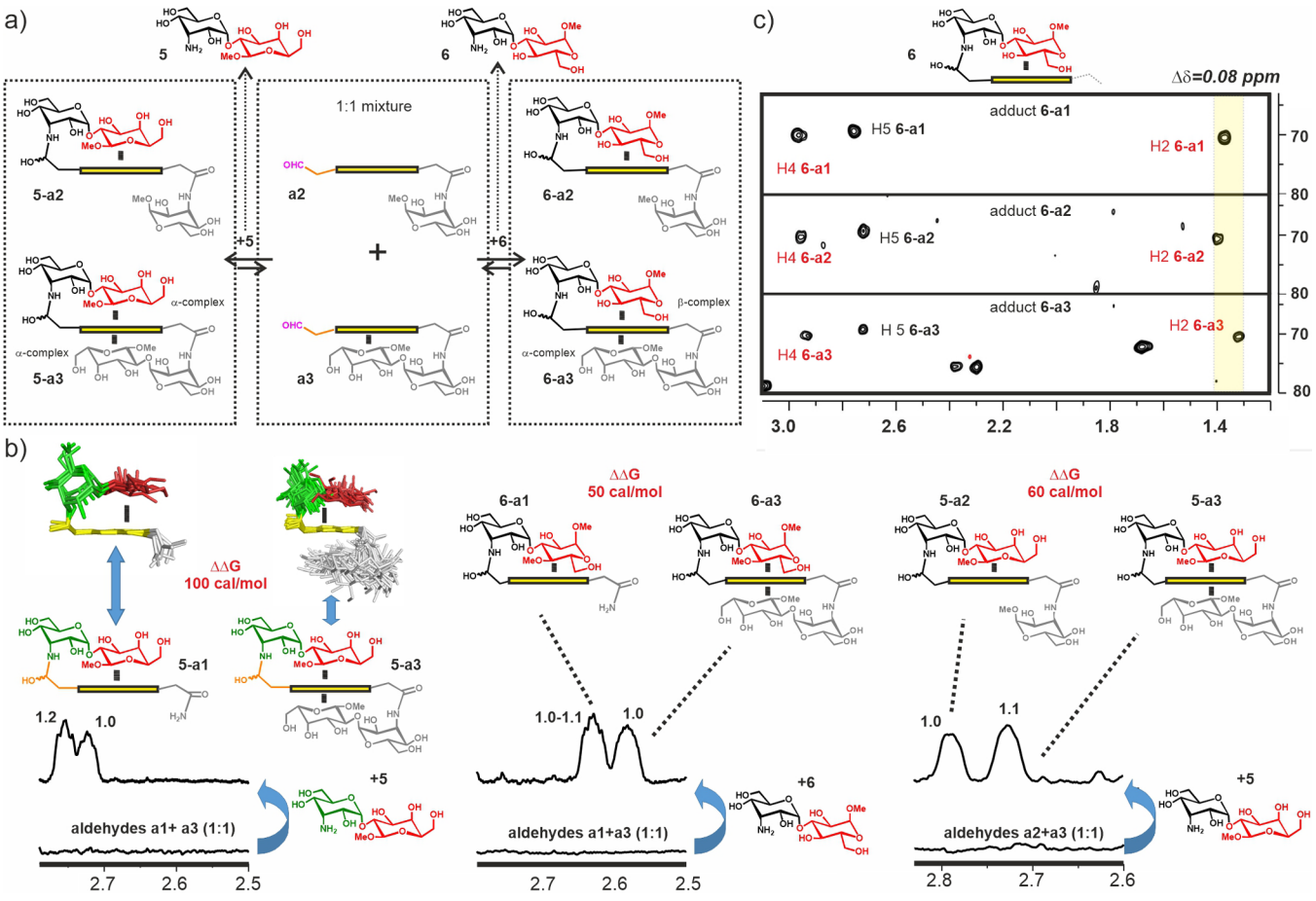

Figure 4. (a) Schematic representation of the dynamic combinatorial experiment designed to evaluate the relative stabilities of CH/π complexes in the context of binary or ternary arrangements. (b) Competitions performed with pairs **a1**/**a3** or **a2**/**a3** and disaccharides **5** or **6** as at 10 °C. Key signals for the final adducts are represented in every case, together with the estimated product ratios (R) and derived free energy differences ($\Delta\Delta G_{cal/mol}$). Molecular dynamics ensembles (explicit water, 1 μs) calculated for adducts **5-a1** and **5-a3** are represented on the left (see also Figure S4). (c) HSQC data sets acquired for hemiaminals **6-a1**, **6-a2** and **6-a3** at 25 °C. Up-field shifted signals for glucose H2 proton are highlighted.

vs **4-A3**). Strikingly, our experiments revealed minor to null differences between identical CH/π bonds within the binary or ternary framework.

CH/π contacts translate in upfield shifted NMR proton signals whose chemical shifts are exquisitely sensitive structural reporters. Taking this into consideration, 2D-NMR experiments were acquired with the final reaction mixtures to derive information about the interaction modes. Thus, Figure 3b shows HSQC data sets acquired with pairs **1**/**2** (top) and **1**/**4** (bottom) after reductive amination with aldehydes **a1** (cyan), **a2** (red) or **a3** (black/gray). Chemical structures for the corresponding secondary amines are represented in Figure 3c. If we look at product **2-A3**, it can be observed that it comprises two stacked galactoses, represented in black and gray, each one involved in CH/π contacts through the α-face. Accordingly, NMR signals for the interacting protons H1, H3 and H5 exhibited highly unusual chemical shifts. For the galactose represented in gray, these amount to 2.9, 1.5, and 2.1 ppm, respectively. Observed δ perturbations are, in all cases, in the $\Delta\delta$ = 1.5−2.0 ppm range, consistent with a fixed and rather stable stacking complex. Interestingly, almost identical $\Delta\delta$ values were detected for the analogous galactose unit present in the unreacted aldehyde **a3**, or in adduct **4-A3** (Figure 3b, bottom-right panel). This almost invariable chemical shift pattern for the interacting galactose hydrogens regardless of the final complex architecture seems to imply that the galactose/naphthyl stacking is, in fact, insensitive to molecular recognition events happening on the other side of the aromatic platform, either solvent-exposed or totally occluded by additional CH/π contacts. Likewise, chemical shift perturbations detected in galactose **2** upon reaction with aldehydes **a1** (cyan), **a2** (red) or **a3** (black) were fairly similar (Figure 3b, top panels), with observed differences among them inferior to 0.2 ppm, pointing to minor geometrical deviations between *binary* or *ternary* complexes. Finally, model **4** products echoed the same behavior (Figure 3b, bottom panels). In summary, these results indicate that *opposite aromatic faces behave as independent noninteracting CH/π acceptor sites both in terms of structure and binding strength.*

To further support this conclusion, we decided to perform additional experiments employing an alternative, more direct approach. The previously described strategy relies on the assumption that the relative population of final secondary amines reflects that of the intermediate hemiaminal/imine/enamine species and, therefore, is not affected by slight differences in the relative reduction rates. Considering the subtle nature of the analyzed effects, we decided to validate this hypothesis by excluding this latter step from our protocol and evaluate directly the relative adduct concentrations in equilibrium. To this end, the scaffold present in disaccharide

https://doi.org/10.1021/jacsau.4c00795
JACS Au 2024, 4, 4466−4473

models **1**−**4** had to be redesigned by inverting position 2 of the amino-altrose unit, from D-altro- to D-allo-configuration. According to our experience,[28] this simple modification allows removing the benzylidene fragment, whose sole purpose was to anchor the D-altropyranose in a $^4C_1$ conformation. More importantly, this inversion enhances the nucleophilicity of the axial amine in position 3 and increases the stability of the hemiaminal species, overall making them now amenable to integration by NMR (at pH > 8.0). This is in contrast with imine or enamine species which remain undetectable (Figure S2).[31]

Another substantial change with our previous protocol is that in this new setup the competing reagents are the corresponding aldehydes, allowing for an orthogonal assessment of the interaction energies. Accordingly, we synthesized disaccharides **5** and **6**, equipped with a β-galactose and an α-glucose as CH/π donor glycosides, respectively. Next, buffered aqueous solutions containing an equimolecular mixture of aldehydes (i.e., **a1**/**a3**) at 10 °C were treated with derivative **5** or **6** to generate a minor fraction of the two hemiaminal derivatives, whose relative populations reflect the strength of the newly established CH/π contacts. This straightforward strategy is outlined in Figures 4a and S3, where example snippets of the performed experiments are shown in Figures 4b and S5−S6. By doing so, we were able to observe that the treatment of an equimolecular **a1**/**a3** mixture with disaccharide **5** leads to the formation of adducts **5-a1** and **5-a3**, with the naphthyl unit partaking in binary and ternary intramolecular CH/π interactions, respectively (no evidence for higher order aggregates was found. Figure S7).

Interestingly, according to NMR data, the single stacking present in **5-a1** was slightly favored over the sandwich-type adduct **5-a3**, suggesting that in the latter a minor interference between stacking contacts could be at work. However, the **5-a1**/**5-a3** equilibrium ratio (1.2/1.0) was consistent with a very minor free energy difference between both species, in the 0.10 kcal/mol range. Similarly, the treatment of pair **a1**/**a3** solution with derivative **6** yielded adducts **6-a1**/**6-a3** with an equilibrium ratio inferior to 1.1, implying a stability difference between complexes lower than 0.05 kcal/mol in favor of the binary stacking (see also Table S2).

Finally, experiments performed with a 1:1 **a2**/**a3** mixture employing disaccharides **5** or **6** yielded almost equimolecular adduct mixtures with a slight excess of **5-a3** and **6-a2**, respectively, in both cases below 10%. According to these assays, CH/π contacts in the context of binary or sandwich-like ternary interactions are nearly isoenergetic. This close equivalence also stems from the geometrical features of the complexes. As an example, Figure 4c shows key HSQC signals of the glucose unit in **6** upon reaction with aldehydes **a1** (**6-a1**), **a2** (**6-a2**) and **a3** (**6-a3**), where the interacting protons H2 and H4 consistently provide upfield shifted cross peaks. In particular, H2 signals exhibit chemical shifts around 1.4 ppm, with $\Delta\delta$ values above −2 ppm. Interestingly, this large perturbation is almost identical for the three adducts, indicating that the carbohydrate/aromatic stacking geometry must remain insensitive to recognition events occurring on the opposite face of the aromatic system (see also Figure S8).

CONCLUSIONS

In summary, herein we report on a dual experimental study based on a dynamic combinatorial strategy capable of revealing very minor stability differences among complexes. The obtained results show insignificant free energy differences between binary and ternary interactions, almost within the detection limit of the employed methodology (<0.05−0.10 kcal/mol), representing less than 10% variation in the overall free energy value. According to this, interactions between stacked glycans mediated by the aromatic unit are indeed negligible.

In our opinion, the lack of cooperativity effects observed in our experiments reflects the distinct nature of CH/π bonds compared to conventional hydrogen bonds, cation/π or anion/π interactions. First, dispersive forces dominate in CH/π contacts, complemented by significant hydrophobic forces, while electrostatic interactions contribute less, even for polarized CH fragments. This contrasts with ion/π interactions, where both electrostatic forces and polarization play a major role, especially with large, polarizable π-surfaces.[22] In addition, CH/π bonds are typically weak, even in water (energy contributions for carbohydrate/aromatic complexes are typically in the 0.5−1.5 kcal/mol),[27] rendering their potential for aromatic polarization limited.

In conclusion, the results of the current study indicate that regarding CH/π bonds, opposite aromatic faces can be deemed as independent binding sites for all practical purposes, making them capable of forming ternary contacts without any associated energy penalty.

MATERIALS AND METHODS

The synthesis of derivatives **1**−**4** has been previously described by our group.[26,27] Regarding compounds **5**−**6** and aldehydes **a1**−**a3** a detailed description of the experimental and synthetic protocols together with the characterization of products and intermediates is included in the Supporting Information.

Dynamic Combinatorial Competition Experiments with Altrosamine Derivatives 1−4

Equimolecular **1**/**2**, **1**/**3** or **1**/**4** mixtures (~1 mM each) in D_2O (10 mM Sodium phosphate) were treated with a substoichiometric amount of either **a1**, **a2** or **a3**. It is worth noting that under the employed pH conditions (pH 6.0) reductive amination is particularly rapid, gradually slowing down under more alkaline conditions. The amount of the aldehyde (300−400 μM) was carefully adjusted to achieve conversions of the altrosamine derivatives inferior to 30%, thus favoring an effective competition of the disaccharide pairs for the aldehyde. After a 1 h equilibration period at 25 °C, sodium cyanoborohydride (5 mM) was added to promote a quick reduction of the imine intermediates. Product formation was followed by 1D-NMR. The final ratio between reduced products was derived by integrating NMR signals in 1D experiments, which were acquired employing long relaxation delays (d1 = 10). For integration purposes, benzylidene nonaromatic CH protons were selected, as they generally provided sharp singlets in well resolved regions of the proton spectra. In particular cases, we resorted to a peak fitting protocol within the Mestre software[32] to allow accurate integration of partially overlapping signals. Product ratios were translated into free energies according to $\Delta G = -RT\mathrm{Ln}(X)$, were X stands for the experimental product ratios.

NMR characterization of the reaction mixtures was accomplished after adding larger quantities of the corresponding aldehydes plus reductive agent, in order to increase the concentration of final products. Both HSQC and TOCSY data sets were acquired with these samples on a Bruker Avance 600 at 25 °C to assign all the CH fragments involved in CH/π interactions with the naphthyl unit.

Dynamic Combinatorial Competition Experiments with Allosamine Derivatives 5−6

Equimolecular **a1**/**a3** or **a2**/**a3** mixtures (1 mM each) in buffered D_2O solutions (10 mM Sodium phosphate, pH 8.2) at 10 °C were

https://doi.org/10.1021/jacsau.4c00795
JACS Au 2024, 4, 4466−4473

treated with an excess of allosamine derivative, **5** or **6**, to generate the corresponding hemiaminals (usually in the 100 μM range), which were characterized by NMR. It should be mentioned that these species are only detectable at pH values greater than 8.0. After a 1 h equilibration period, adduct ratios, formally equivalent to the thermodynamic equilibrium constant for adduct exchange, were derived by integrating NMR signals in 1D experiments acquired with long relaxation delays (d1 = 10). For integration purposes, we selected galactose or allosamine H5 protons (for **5** and **6** adducts, respectively), as they provided, in most cases, well-resolved non-overlapping peaks. HSQC and TOCSY data sets were acquired with the final mixtures on a Bruker Avance 600 at 10 °C to assign all the CH fragments involved contacts with the aromatic platform. Equilibrium constants (K_{eq}) were translated in free energy values according to the Gibbs equation $\Delta G = -RT\mathrm{Ln}(K_{eq})$.

It is important to note that inorganic cations have no discernible effect on the strength of the analyzed CH/π interactions at the employed buffer concentration (see experiments performed with different amounts of sodium chloride in Figure S9).

Molecular Dynamics (MD) Simulations

MD trajectories for the alternative hemiaminal adducts were collected as previously described.[6]

■ ASSOCIATED CONTENT

Supporting Information

The Supporting Information is available free of charge at https://pubs.acs.org/doi/10.1021/jacsau.4c00795.

Detailed description of the experimental methods and synthetic protocols together with the characterization of products and intermediates; Figures S1−S9: details of the NMR reactivity experiments and MD calculations (PDF)

■ AUTHOR INFORMATION

Corresponding Author

Juan Luis Asensio − *Instituto de Química Orgánica General (IQOG-CSIC), 28006 Madrid, Spain;* orcid.org/0000-0001-7536-5221; Email: iqoa110@iqog.csic.es

Authors

Laura Díaz-Casado − *Instituto de Química Orgánica General (IQOG-CSIC), 28006 Madrid, Spain*

Enrique Mann − *Instituto de Química Orgánica General (IQOG-CSIC), 28006 Madrid, Spain*

Ester Jiménez-Moreno − *Instituto de Química Orgánica General (IQOG-CSIC), 28006 Madrid, Spain*

Alejandro Villacampa − *Instituto de Química Orgánica General (IQOG-CSIC), 28006 Madrid, Spain*

Laura Montalvillo-Jiménez − *Instituto de Química Orgánica General (IQOG-CSIC), 28006 Madrid, Spain*

Claudia Sánchez-García − *Instituto de Química Orgánica General (IQOG-CSIC), 28006 Madrid, Spain*

Francisco Corzana − *Dept. Química and Centro de Investigación en Síntesis Química, Universidad de La Rioja, 26006 La Rioja, Spain;* orcid.org/0000-0001-5597-8127

Jesús Jiménez-Barbero − *Center for Cooperative Research in Biosciences (CIC bioGUNE), Basque Research and Technology Alliance (BRTA), 48160 Derio, Bizkaia, Spain; Ikerbasque, Basque Foundation for Science, 48009 Bilbao, Spain; Centro de Investigacion Biomedica En Red de Enfermedades Respiratorias, 28029 Madrid, Spain;* orcid.org/0000-0001-5421-8513

Ana María Gómez − *Instituto de Química Orgánica General (IQOG-CSIC), 28006 Madrid, Spain;* orcid.org/0000-0002-8703-3360

Andrés G. Santana − *Instituto de Productos Naturales y Agrobiología (IPNA-CSIC), 38206 San Cristobal de la Laguna, Tenerife, Spain;* orcid.org/0000-0003-3568-7714

Complete contact information is available at: https://pubs.acs.org/10.1021/jacsau.4c00795

Author Contributions

CRediT: **L.D.-C.** investigation, methodology; **E.M.** investigation; **E.J.-M.** investigation, methodology; **A.V.** investigation; **L.M.-J.** investigation; **C.S.-G.** investigation; **F.C.** investigation, resources, writing - review & editing; **J.J.-B.** resources, writing - review & editing; **A.M.G.** resources, writing - review & editing; **A.G.S.** investigation, methodology, writing - original draft, writing - review & editing; **J.L.A.** conceptualization, funding acquisition, supervision, writing - original draft, writing - review & editing.

Notes

The authors declare no competing financial interest.

■ ACKNOWLEDGMENTS

This investigation was supported by research grant PID2022-141085NB-I00 funded by MCIN/AEI/10.13039/501100011033 and by ERDF A way of making Europe. A.G.S. thanks grant RYC2021-031704-I funded by MCIN/AEI/10.13039/501100011033 and by European Union NextGeneration EU/PRTR. L.D.-C., A.V. and C.S.-G. thank grants BES-2017-080618, PRE2020-093392 and PREP2022-000224, respectively, funded by MCIN/AEI/10.13039/501100011033.

■ REFERENCES

(1) Johnson, D. W.; Hof, F., Eds. *Aromatic Interactions: Frontiers in Knowledge and Application*; The Royal Society of Chemistry: Cambridge, 2017.

(2) Zhao, Y.; Cotelle, Y.; Sakai, N.; Matile, S. Unorthodox Interactions at Work. *J. Am. Chem. Soc.* **2016**, *138*, 4270−4277.

(3) Nishio, M.; Hirota, M.; Umezawa, Y. *The CH/π interaction. Evidence, Nature, and Consequences*; Wiley-VCH: New York, 1998.

(4) Platzer, G.; Mayer, M.; Beier, A.; Brüschweiler, S.; Fuchs, J. E.; Engelhardt, H.; Geist, L.; Bader, G.; Schörghuber, J.; Lichtenecker, R.; Wolkerstorfer, B.; Kessler, D.; McConnell, D. B.; Konrat, R. PI by NMR: Probing CH−π Interactions in Protein−Ligand Complexes by NMR Spectroscopy. *Angew. Chem., Int. Ed.* **2020**, *59*, 14861−14868.

(5) Krone, M. W.; Travis, C. R.; Lee, G. Y.; Eckvahl, H. J.; Houk, K. N.; Waters, M. L. More Than π−π−π Stacking: Contribution of Amide−π and CH−π Interactions to Crotonyllysine Binding by the AF9 YEATS Domain. *J. Am. Chem. Soc.* **2020**, *142*, 17048−17056.

(6) Díaz-Casado, L.; Villacampa, A.; Corzana, F.; Jiménez-Barbero, J.; Gómez, A. M.; Santana, A. G.; Asensio, J. L. Illuminating a Solvent-Dependent Hierarchy for Aromatic CH/π Complexes with Dynamic Covalent Glyco-Balances. *JACS Au* **2024**, *4*, 476−490.

(7) Nishio, M.; Umezawa, Y.; Fantini, J.; Weiss, M. S.; Chakrabarti, P. CH−π hydrogen bonds in biological macromolecules. *Phys. Chem. Chem. Phys.* **2014**, *16*, 12648−12683.

(8) Chung, M. K.; White, P. S.; Lee, S. J.; Waters, M. L.; Gagné, M. R. Self-Assembled Multi-Component Catenanes: Structural Insights into an Adaptable Class of Molecular Receptors and [2]-Catenanes. *J. Am. Chem. Soc.* **2012**, *134*, 11415−11429.

(9) Ke, C.; Destecroix, H.; Crump, M. P.; Davis, A. P. A simple and accessible synthetic lectin for glucose recognition and sensing. *Nat. Chem.* **2012**, *4*, 718−723.
(10) Somovilla, V. J.; Bermejo, I. A.; Albuquerque, I. S.; Martínez-Sáez, N.; Castro-López, J.; García-Martín, F.; Compañón, I.; Hinou, H.; Nishimura, S.-I.; Jiménez-Barbero, J.; Asensio, J. L.; Avenoza, A.; Busto, J. H.; Hurtado-Guerrero, R.; Peregrina, J. M.; Bernardes, G. J. L.; Corzana, F. The Use of Fluoroproline in MUC1 Antigen Enables Efficient Detection of Antibodies in Patients with Prostate Cancer. *J. Am. Chem. Soc.* **2017**, *139*, 18255−18261.
(11) Ozawa, T.; Tsuji, E.; Ozawa, M.; Handa, C.; Mukaiyama, H.; Nishimura, T.; Kobayashi, S.; Okazaki, K. The importance of CH/π hydrogen bonds in rational drug design: An ab initio fragment molecular orbital study to leukocyte-specific protein tyrosine (LCK) kinase. *Bioorg. Med. Chem.* **2008**, *16*, 10311−10318.
(12) Samaroo, S.; Hengesbach, C.; Bruggeman, C.; Carducci, N. G. G.; Mtemeri, L.; Staples, R. J.; Guarr, T.; Hickey, D. P. C−H···π interactions disrupt electrostatic interactions between non-aqueous electrolytes to increase solubility. *Nat. Chem.* **2023**, *15*, 1365−1373.
(13) Sozzani, P.; Comotti, A.; Bracco, S.; Simonutti, R. A Family of Supramolecular Frameworks of Polyconjugated Molecules Hosted in Aromatic Nanochannels. *Angew. Chem., Int. Ed.* **2004**, *43*, 2792−2797.
(14) Neel, A. J.; Hilton, M. J.; Sigman, M. S.; Toste, F. D. Exploiting non-covalent π interactions for catalyst design. *Nature* **2017**, *543*, 636−646.
(15) Montalvillo-Jiménez, L.; Santana, A. G.; Corzana, F.; Jiménez-Osés, G.; Jiménez-Barbero, J.; Gómez, A. M.; Asensio, J. L. Impact of Aromatic Stacking on Glycoside Reactivity: Balancing CH/π and Cation/π Interactions for the Stabilization of Glycosyl-Oxocarbenium Ions. *J. Am. Chem. Soc.* **2019**, *141*, 13372−13384.
(16) Brandl, M.; Weiss, M. S.; Jabs, A.; Suehnel, J.; Hilgenfeld, R. C-H···pi-interactions in proteins. *J. Mol. Biol.* **2001**, *307*, 357−377.
(17) Asensio, J. L.; Ardá, A.; Cañada, F. J.; Jiménez-Barbero, J. Carbohydrate−Aromatic Interactions. *Acc. Chem. Res.* **2013**, *46*, 946−954.
(18) Mahadevi, A. S.; Sastry, G. N. Cooperativity in Noncovalent Interactions. *Chem. Rev.* **2016**, *116*, 2775−2825.
(19) von Krbek, L. K. S.; Schalley, C. A.; Thordarson, P. Assessing cooperativity in supramolecular systems. *Chem. Soc. Rev.* **2017**, *46*, 2622−2637.
(20) Trevisan, L.; Bond, A. D.; Hunter, C. A. Quantitative Measurement of Cooperativity in H-Bonded Networks. *J. Am. Chem. Soc.* **2022**, *144*, 19499−19507.
(21) Vijay, D.; Sastry, G. N. The cooperativity of cation−π and π−π interactions. *Chem. Phys. Lett.* **2010**, *485*, 235−242.
(22) Bornhof, A.-B.; Bauzá, A.; Aster, A.; Pupier, M.; Frontera, A.; Vauthey, E.; Sakai, N.; Matile, S. Synergistic Anion−(π)n−π Catalysis on π-Stacked Foldamers. *J. Am. Chem. Soc.* **2018**, *140*, 4884−4892.
(23) Zhao, C.; Li, P.; Smith, M. D.; Pellechia, P. J.; Shimizu, K. D. Experimental Study of the Cooperativity of CH−π Interactions. *Org. Lett.* **2014**, *16*, 3520−3523.
(24) Hudson, K. L.; Bartlett, G. J.; Diehl, R. C.; Agirre, J.; Gallagher, T.; Kiessling, L. L.; Woolfson, D. N. Carbohydrate−Aromatic Interactions in Proteins. *J. Am. Chem. Soc.* **2015**, *137*, 15152−15160.
(25) Ardejani, M. S.; Noodleman, L.; Powers, E. T.; Kelly, J. W. Stereoelectronic effects in stabilizing protein−N-glycan interactions revealed by experiment and machine learning. *Nat. Chem.* **2021**, *13*, 480−487.
(26) Santana, A. G.; Jiménez-Moreno, E.; Gómez, A. M.; Corzana, F.; González, C.; Jiménez-Osés, G.; Jiménez-Barbero, J.; Asensio, J. L. A Dynamic Combinatorial Approach for the Analysis of Weak Carbohydrate/Aromatic Complexes: Dissecting Facial Selectivity in CH/π Stacking Interactions. *J. Am. Chem. Soc.* **2013**, *135*, 3347−3350.
(27) Jiménez-Moreno, E.; Jiménez-Osés, G.; Gómez, A. M.; Santana, A. G.; Corzana, F.; Bastida, A.; Jiménez-Barbero, J.; Asensio, J. L. A thorough experimental study of CH/π interactions in water: quantitative structure−stability relationships for carbohydrate/aromatic complexes. *Chem. Sci.* **2015**, *6*, 6076−6085.
(28) Jiménez-Moreno, E.; Gómez, A. M.; Bastida, A.; Corzana, F.; Jiménez-Osés, G.; Jiménez-Barbero, J.; Asensio, J. L. Modulating Weak Interactions for Molecular Recognition: A Dynamic Combinatorial Analysis for Assessing the Contribution of Electrostatics to the Stability of CH−π Bonds in Water. *Angew. Chem., Int. Ed.* **2015**, *54*, 4344−4348.
(29) Cougnon, F. B. L.; Sanders, J. K. M. Evolution of dynamic combinatorial chemistry. *Acc. Chem. Res.* **2012**, *45* (12), 2211−2221.
(30) Corbett, P. T.; Leclaire, J.; Vial, L.; West, K. R.; Wietor, J.-L.; Sanders, J. K. M.; Otto, S. Dynamic Combinatorial Chemistry. *Chem. Rev.* **2006**, *106* (9), 3652−3711.
(31) The relatively lower stability of the imine derivative compared to the hemiaminal can be rationalized by repulsive interactions between the nitrogen atom and the axially oriented α-anomeric substituent. Furthermore, hydrogen bonding interactions have been demonstrated to play a significant role in modulating hemiaminal/imine/enamine equilibria. It should be noted that, in our case, hemiaminals can be further stabilized by intramolecular hydrogen bonding with hydroxyl groups at either positions C2 or C4 of the pyranose ring.
(32) MestRe Nova. *Mestrelab Research S.L. Feliciano Barrera 9B, Bajo, 15706 Santiago de Compostela, Spain*. http://www.mestrelab.com.

https://doi.org/10.1021/jacsau.4c00795
JACS Au 2024, 4, 4466−4473